Rheology and Viscosity Scaling of the Polyelectrolyte Xanthan Gum

Nicholas B. Wyatt, Matthew W. Liberatore

Department of Chemical Engineering, Colorado School of Mines, Golden 80401, Colorado

Received 8 April 2009; accepted 10 July 2009
DOI 10.1002/app.31093
Published online 19 August 2009 in Wiley InterScience (www.interscience.wiley.com).

ABSTRACT: The viscosity as a function of concentration for xanthan gum in both salt-free solution and in 50 m*M* NaCl is measured and compared with a scaling theory for polyelectrolytes. In general, the zero shear rate viscosity and the degree of shear thinning increase with polymer concentration. In addition, shear thinning was observed in the dilute regime in both solvents. In salt-free solution, four concentration regimes of viscosity scaling and three associated critical concentrations were observed ($c^* \approx$ 70 ppm, $c_e \approx 400$ ppm, and $c_D \approx 2000$ ppm). In salt solution, only three concentration regimes and two critical concentrations were observed ($c^* \approx 200$ ppm and $c_e \approx 800$ ppm). In the presence of salt, the polymer chain structure collapses and occupies much less space resulting in higher values of the critical concentrations. The observed viscosity-concentration scaling is in very good agreement with theory in the semidilute unentangled and semidilute entangled regimes in both salt-free and 50 m*M* NaCl solution. © 2009 Wiley Periodicals, Inc. J Appl Polym Sci 114: 4076–4084, 2009

Key words: biopolymers; polyelectrolytes; rheology

INTRODUCTION

Charged polymer systems are encountered daily in nature as many biological polymers, such as DNA, are polyelectrolytes. Polyelectrolytes are used extensively in many industrial applications such as food additives, flocculants, drilling fluids, and drag reducers. Because polyelectrolytes are such an important part of so many different systems and industries, a fundamental understanding of the rheology of polyelectrolyte solutions is critical.

Xanthan gum is a high molecular weight, anionic, extracellular polysaccharide produced by the bacterium Xanthomonas campestris.[1] The primary structure of xanthan consists of a β-1,4-linked glucan backbone with charged trisaccharide side chains (β-D-mannopyrannosyl-(1,4)-α-D-glucopyrannosyl-(1,2)-β-D-mannopyrannosyl-6-O-acetate) on alternating backbone residues (Fig. 1).[2,3] Variations in processing procedures and conditions lead to varying degrees of acetyl substitution (of the mannose residues adjacent to the backbone) and pyruvic acetal substitution (of the terminal mannose units). The variations in degrees of substitution on the side chains have been shown to affect the rheological properties of the polymer.[4,5] The primary industrial applications for xanthan gum are viscosity modification and stabilization in food products (i.e., salad dressing, ice cream, yogurt) and personal care products (i.e., lotions, creams, body washes), drilling fluids for enhanced oil recovery, drug delivery, and drag reduction.[3,6–12] The global market for xanthan is ~ $500 million annually and continues to grow.

Xanthan solution properties have been studied extensively over the past 40 years.[3,7,9,13–29] The main topics of interest have included solution viscosity, polymer conformation, temperature effects on polymer conformation, and the effects of salt on both solution properties and chain conformation. Xanthan exhibits both anisotropic and isotropic phases in solution.[24–27] The relative amount of each phase present in solution depends on the polymer molecular weight, polymer concentration, and solution ionic strength. The highest concentration used here remains well below the biphasic regime. Further, xanthan has been shown to exhibit two different conformational states: an ordered, helical conformation and a disordered conformation that can be described as a broken or imperfect helix.[2,17,21] The conformation assumed by the xanthan molecules is highly dependent on the ionic content of the solvent. In salt-free solution, the xanthan backbone is disordered and highly extended due to electrostatic repulsions between charges on the side chains. In this state, the chains are relatively stiff, but retain some degree of flexibility. When salt ions are present in solution, the ordered, helical conformation is stabilized. Xanthan chains in the helical conformation

Correspondence to: M. W. Liberatore (mliberat@mines.edu).

Contract grant sponsor: Donors of the American Chemical Society Petroleum Research Fund.

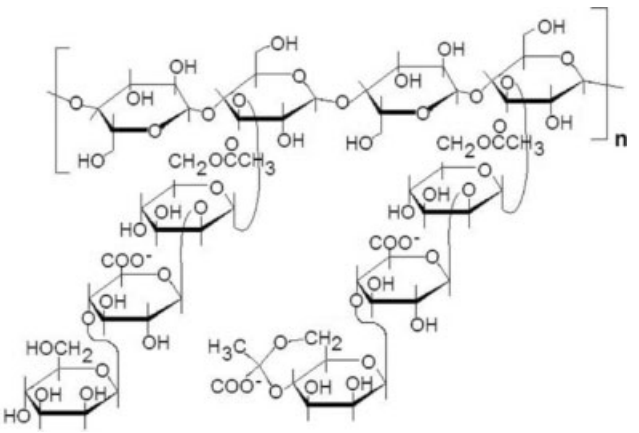

Figure 1 Molecular structure of xanthan according to Jansson et al.[2]

are much more rigid than the disordered chains and have been shown to have a persistence length similar to that of double stranded DNA.

Several studies have reported values, both experimental and predicted, of critical concentrations of varying definitions. However, a comprehensive study of solution viscosity, critical concentrations, and the effects of added salt on both the viscosity and critical concentrations for solutions from dilute to entangled does not exist. In the current study, this void is filled by experimentally deriving values for the overlap (c^*) and entanglement (c_e) concentrations for isotropic solutions in both salt-free and 50 m*M* NaCl solution. Scaling observations of the zero shear rate viscosity and characteristic relaxation time for xanthan solutions are also compared with a theory proposed by Dobrynin et al.[30]

Polyelectrolyte solution rheology is complex because of the sensitivity of the polymer to the presence of ions in solution.[31–41] Several theories have been proposed to explain the observed differences in properties between polyelectrolytes and neutral polymers.[30,42–47] According to the theory proposed by Dobrynin et al.[30,43] polyelectrolyte chains can be represented as a chain of electrostatic blobs. The blobs repel each other resulting in a fully extended chain of electrostatic blobs. The chain conformation within the electrostatic blob is essentially independent of electrostatic interactions and depends solely on the thermodynamic interactions between uncharged polymer and solvent. The dynamics of the polymer chain within the electrostatic blobs are described as Zimm like, whereas the dynamics of the chain outside the blob are Rouse like. The polymer chain remains rodlike up to the correlation length (ξ), the distance over which fluctuations in a system are correlated. For length scales larger than ξ, the chain becomes flexible and is described by a random walk of correlation blobs, which are composed of rodlike assemblies of electrostatic blobs. The flexibility on length scales larger than the correlation length is due to the charge screening of surrounding chains in solution.

Using this conceptual picture of polyelectrolye chain behavior, several scaling regimes for the zero shear rate viscosity (η_0) and characteristic relaxation time (τ) for flexible polyelectrolytes in salt-free solution were proposed.[30] Although scaling theories are stated to apply to flexible polyelectrolytes, the polymer persistence length, or other characteristics of chain stiffness do not appear within the theory.[30,43,48] When the polyelectrolyte concentration exceeds the overlap concentration (c^*), η_0 is proportional to the square root of concentration ($\eta_0 \sim c^{1/2}$), in agreement with the phenomenological law proposed by Fuoss.[33,49] Empirically, the overlap concentration generally occurs at about twice the solvent viscosity (η_s) in polyelectrolyte solutions.[30] The semidilute unentangled regime is predicted to be very wide, spanning three to four decades in polymer concentration ($c_e = 10^3 c^*$). The large span of the semidilute unentangled regime is attributed to the stronger concentration dependence on chain size ($R \sim c^{-1/4}$ as opposed to $R \sim c^{-1/8}$ for neutral polymers)[30] coupled with the need for each polymer chain to overlap n others to become entangled. For concentrations above c_e, the proportionality increases to $\eta_0 \sim c^{3/2}$. For polyelectrolyte solutions, a certain concentration c_D exists where the electrostatic blobs begin to overlap. Above c_D, the viscosity scaling is predicted to be the same as for uncharged polymers in good or Θ solvents ($\eta_0 \sim c^{15/4}$ or $\eta_0 \sim c^{14/3}$).

In the present work, scaling of zero shear rate viscosity of xanthan with concentration and the theory proposed by Dobrynin et al. are compared over a range of concentration from 10 to 6000 parts per million by weight (ppm). Further, viscosity, critical concentrations, relaxation times, and dynamic moduli are reported for xanthan in both salt-free solution and in 50 m*M* NaCl.

MATERIALS AND METHODS

Materials

The xanthan gum used in the current study is a commercial, food grade polymer (Keltrol T 622, Mat. # 20000625) donated by CP Kelco in powder form. The xanthan has an estimated molecular weight of 2 $\times$ 106 Da and polydispersity index of $\sim$ 2. The manufacturer reports that the product is "clarifed," meaning extra steps were taken to remove residual cellular debris from the fermentation process. Solutions with concentrations up to 10,000 ppm have been made and observed to be optically clear. The powder was used as received without further purification or modification. For comparison, a quantity of

the xanthan used here was dialyzed exhaustively to obtain the potassium salt form. The rheology of the dialyzed xanthan agreed to within experimental error and errors expected from batch to batch variation in xanthan products. Deionized water was obtained by passing house deionized water through a Barnstead NANOpure Diamond UV ultrapure water system followed by a 0.2-μm filter. The resulting deionized water had a measured resistance of 18.2 MΩ cm. The reagent grade NaCl used was obtained from Mallinckrodt Chemicals (Product #7581-12) and was used without further purification. The glassware used for mixing and storage of xanthan solutions was carefully cleaned with either ethanol or acetone (reagent grade), then rinsed with purified deionized water to remove all traces of salt.

Sample preparation

Xanthan solutions were prepared by dissolving the polymer powder in either deionized water (salt-free solution, i.e., no added salt) or 50 m*M* NaCl. The solutions were stirred using a magnetic stir bar for $\sim$ 1 h, allowed to rest for $\sim$ 24 h at room temperature, and finally used for rheological testing. Several samples were prepared by adding NaCl to a xanthan solution to compare the resulting rheological properties to solutions prepared by adding xanthan powder to a NaCl solution. No measurable differences in viscosity or dynamic moduli were observed when comparing the sample preparation methods. In all cases, measurements were made 1–4 days after solution preparation. In the period of 1–4 days after sample preparation, no measurable change in rheological properties of the solutions was observed. The solutions were discarded 6 days after preparation as polymer degradation became evident (e.g., significant decrease in viscosity and loss of optical clarity).

Rheology

All rheological data were collected using a TA Instruments AR-G2 stress controlled rheometer. Experiments were conducted using either a stainless steel cone (60-mm diameter, 1 degree) and plate or a concentric cylinder (Couette cell) geometry (of outer diameter 30.0 mm and inner diameter 28.0 mm) in steady or oscillatory shear. Sample evaporation was minimized by using a solvent trap in conjunction with the appropriate geometry. Temperature was controlled at 25.0 $\pm$ 0.1°C using a Peltier plate (cone and plate) or a Peltier jacket (Couette). Calibration with viscosity standard oils showed agreement with an error of <3%. The AR-G2 rheometer has a torque range of 0.01–200 mN·m, which is sufficiently sensitive to measure zero shear rate viscosities at very low polymer concentrations ($c < 10$ ppm).

The data reported here are the averages of at least three replicate data sets and the associated error bars represent one standard deviation unless otherwise noted.

RESULTS AND DISCUSSION

Salt-free solution

Xanthan solutions in the absence of salt exhibit a newtonian plateau and shear thinning behavior typical of polymer solutions (Fig. 2). Below 20 ppm, the xanthan solutions behave like newtonian solutions. Of note, shear thinning behavior was observed for xanthan concentrations in the dilute regime (20 ppm $< c <$ 70 ppm). Representative flow curves from each of the four concentration regimes (Fig. 2) are described well by the Cross model,

$$\eta = \frac{\eta_0 - \eta_\infty}{1 + (K\dot{\gamma})^m} + \eta_\infty$$

where η_0 is the zero shear rate viscosity, η_∞ is the infinite shear rate viscosity, K is the characteristic time of the solution, and m is the rate index. As expected, η_0 increases monotonically with xanthan concentration and η_∞ for all concentrations is near the solvent viscosity (Table I). Further, a power law of the form

$$\eta = A\dot{\gamma}^n$$

fit to the shear thinning region shows that the degree of shear thinning (quantified by the power law index, n; Table I) increases with polyelectrolyte concentration.

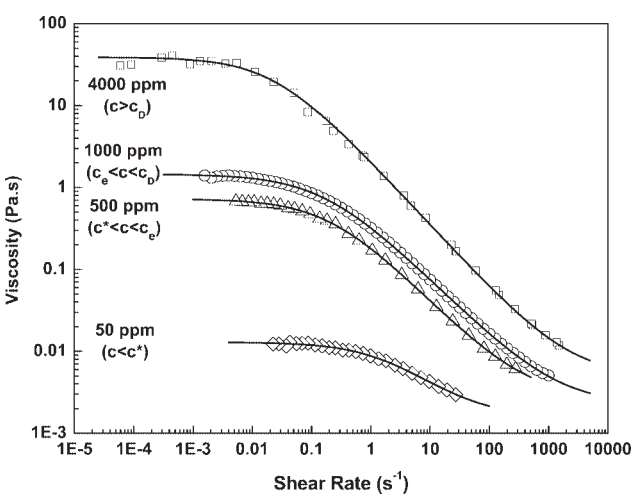

Figure 2 Viscosity as a function of shear rate for several xanthan concentrations in salt-free solution. Solid lines are Cross model fits to the measured points.

TABLE I
Fit Parameters for Cross and Power Law Models for Several Xanthan Concentrations

Concentration (ppm)	η_0 (Pa s)	η_∞ (Pa s)	K (s)	m	n
4000	39	5.1×10^{-3}	41	0.78	−0.72
1000	1.5	2.3×10^{-3}	5.8	0.73	−0.61
200	0.33	3.1×10^{-3}	4.8	0.78	−0.58
50	0.01	1.6×10^{-3}	0.49	0.76	−0.34

Using a set of 30 flow curves (four representative examples are shown in Fig. 2), the critical concentrations for xanthan were determined from the dependence of zero shear rate viscosity on polyelectrolyte concentration. Over a range of three decades of xanthan concentration, four distinct regions of viscosity scaling show very good agreement with the theory proposed by Dobrynin et al. (Fig. 3). The overlap concentration ($c^* \approx 70$ ppm) is characterized by a sudden increase (by a factor of ~ 5) in η_0 over a narrow range in concentration (~ 15 ppm). The increase is attributed to the fact that as the number of polyelectrolyte chains in solution increases, the space between the chains (and therefore the anionic charges on the chains) decreases. As the charges get closer to one another, the repulsive forces between the chains increase. Thus, there is an increase in the resistance of the chains when trying to move past one another leading to the observed increase in viscosity. Empirically, c^* usually occurs at about twice the viscosity of the solvent (0.00088 Pa s, in this case). However, the viscosity at c^* for xanthan is ~ 90 times larger than the solvent viscosity. It is interesting to note that for dilute solutions, η_0 scales with concentration to a degree ($\eta \sim c^{1.6}$) that is very close to the scaling observed in the semidilute entangled regime ($\eta \sim c^{1.5}$).

In the semidilute unentangled regime ($c^* < c < c_e$), η_0 increases as the square root of polyelectrolyte concentration, which is a weaker concentration dependence than for neutral polymers ($\eta_0 \sim c$ in Θ solvent). The entire semidilute unentangled regime is well described by the empirical Fuoss law ($\eta_0 \sim c^{1/2}$). Unlike the three to four decades in concentration that the semidilute unentangled region is predicted to span, this region is found to be relatively small for xanthan, spanning less than one decade in concentration ($c^* \approx 70$ ppm to $c_e \approx 400$ ppm).

Further agreement with theory is shown in the semidilute entangled regime, where η_0 was found to scale as $c^{3/2}$. The dependence of viscosity on polyelectrolyte concentration in the semidilute entangled regime is much weaker than the neutral polymer case ($\eta \sim c^{15/4}$ in good solvents and $\eta \sim c^{14/3}$ in Θ solvents). Also, the entanglement concentration is evidenced by a minimum in a plot of the reduced viscosity η_R [where $\eta_R = (\eta - \eta_s)/\eta_s c$] versus polymer concentration (not shown).

The final critical concentration (c_D) and associated increase in viscosity is observed at around 2000 ppm. Dobrynin et al. defined c_D as the concentration at which electrostatic blobs begin to overlap. A crossover in viscosity behavior is predicted to occur at c_D where the behavior changes from that of charged polymers to neutral polymers in good or Θ solvents. For concentrations above c_D, the electrostatic blob concept breaks down, and the solution rheology is due mainly to the polymeric nature of the polyelectrolyte solution.[30] In this study, η_0 was observed to scale to the power of 15/4 above c_D, which is identical to the scaling predicted for neutral polymers in good solvents. Therefore, our observations confirm the crossover to neutral polymer behavior in this concentration region.

Although the theory proposed by Dobrynin et al. is based on flexible polyelectrolytes, we show remarkable agreement for xanthan, which has been shown to be rather rigid. Several studies report the persistence length of xanthan to be 100–150 nm in salt solution.[10,50–52] Double-stranded DNA has a persistence length of ~ 50 nm in salt solution.[48] A recent study reports the persistence length of short-chain branched polyethylene (a flexible polymer) in solution to be ~ 0.8 nm.[53] Although most studies report persistence lengths for xanthan in an ionic solution, it is clear that xanthan retains a high degree of rigidity in salt-free solution. The role of chain flexibility in the scaling theory is unclear; however, our data suggest that scaling principles may successfully be applied to rigid polyelectrolyte systems.

Comparing the measured shear viscosity with the dynamic viscosity indicates that the well known

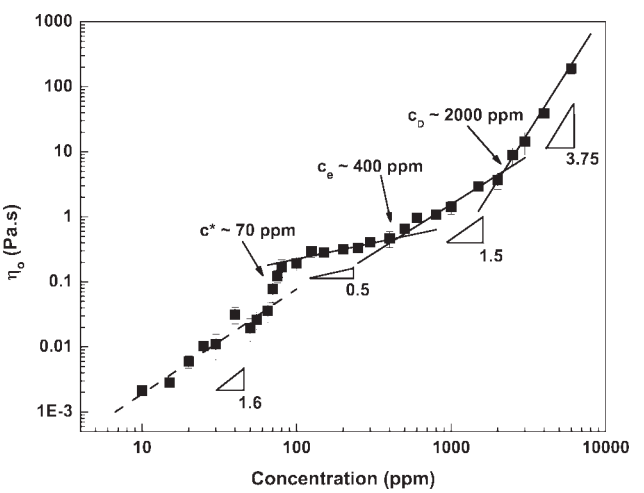

Figure 3 Zero shear rate viscosity scaling as a function of xanthan concentration in salt-free solution. Solid lines indicate theoretical scaling for $c > c^*$ and dashed line represents a power law fit below c^*.

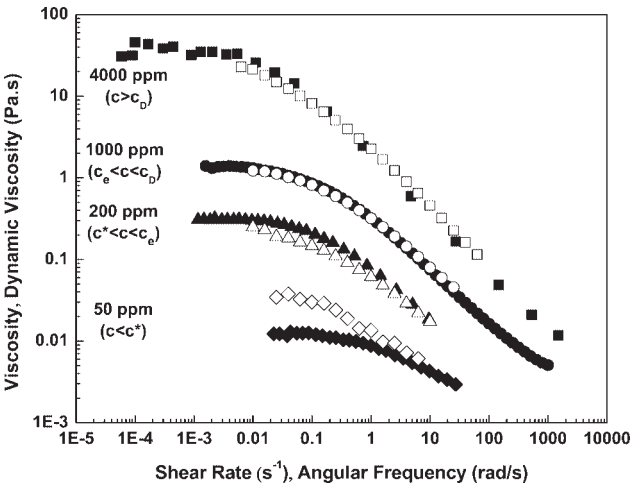

Figure 4 Comparison of the dynamic viscosity (open symbols) with the shear viscosity (closed symbols) for several xanthan concentrations.

Cox-Merz rule applies to the xanthan solutions studied here for all but the lowest concentrations (Fig. 4). The validity of the Cox-Merz rule observed seems to disagree with previous studies that have shown that the Cox-Merz rule does not hold for xanthan.[25,54] The discrepancy is likely due to the concentration of the xanthan solutions used. According to the phase diagram given by Inatomi et al.,[27] the solutions where the Cox-Merz rule does not apply lie in either the biphasic or anisotropic regime while all solutions in the present work lie in the isotropic regime.

The dynamic moduli provide additional information on the viscoelastic nature of the xanthan solutions in the four concentration regimes (Fig. 5). In the dilute limit [Fig. 5(b)], the storage modulus (G′) tends to zero (i.e., newtonian fluid) as the concentration decreases. As the polymer concentration is increased, a crossover in G′ and G″ is observed [Fig. 5(a)]. The crossover in G′ and G″ signifies the crossover from more liquid like to more elastic behavior. The inverse of the crossover frequency is directly related to a relaxation time for the polyelectrolyte.

The dependence of the relaxation time (τ) on polymer concentration for polyelectrolytes differs greatly from neutral polymer behavior. Dobrynin et al. predict that the relaxation time decreases with polymer concentration (scaling as $c^{-1/2}$) for the semidilute unentangled regime, and the relaxation time in the semidilute entangled regime is predicted to be independent of polymer concentration. For neutral polymers, τ is expected to increase with concentration for all concentrations.

To further compare the experimental observations for xanthan with theoretical predictions, relaxation times were determined from the measured rheological data. Following the method of Boris et al.,[55] the characteristic relaxation time (τ) was determined from the viscosity verses shear rate data by determining the intersection of the power law fit to the shear thinning regime and the least squares fit to the newtonian plateau. The reciprocal of the shear rate at which the power law fit and the least squares fit intersect gives a characteristic relaxation time. Four distinct scaling regions in the dependence of the characteristic relaxation time on the polyelectrolyte concentration in salt-free solution are observed (Fig. 6). In the semidilute unentangled regime, the relaxation time decreases with increasing polymer concentration ($\tau \sim c^{-1/2}$) whereas in the semidilute entangled regime, the relaxation time is independent of polymer concentration. Therefore, very good agreement with theory was found in the range $c^* < c < c_D$.

Published theories do not explain the relaxation time dependencies observed in salt-free solution in the concentration ranges below c^* or above c_D. For the xanthan solutions studied here, relaxation time increases with concentration as $\sim c^{3/2}$ in the dilute

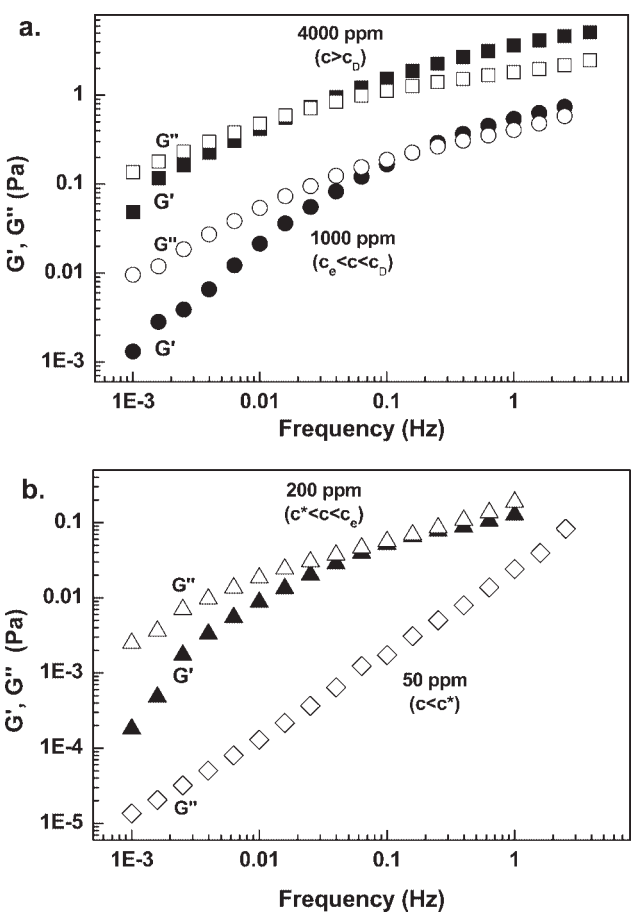

Figure 5 Dynamic mechanical properties (G′ filled, G″ open) as a function of frequency for (a) one concentration above c_D and one concentration in the semidilute entangled regime and (b) one concentration in the semidilute unentangled regime and one concentration in the dilute regime in salt-free solution.

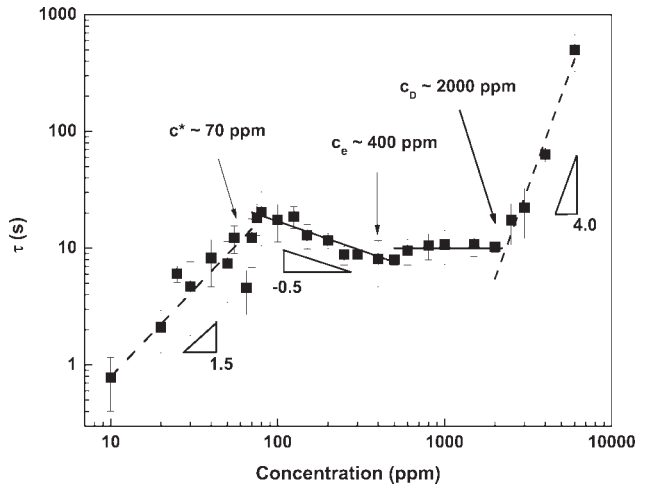

Figure 6 Dependence of relaxation time on xanthan concentration in salt-free solution. Solid lines show scaling predicted by theory ($c^* < c < c_D$) whereas dashed lines are power law fits. Critical concentrations were determined from Figure 3.

regime, which is the expected result for a neutral polymer in the entangled regime. Further, as the polymer concentration is increased, a maximum in the relaxation time was observed at low polymer concentration (near c^*) followed by a decrease into the semidilute unentangled regime. Similar behavior has been observed in other polyelectrolyte solutions,[55,56] but is not described by theory. In addition, the scaling of τ in the dilute regime agrees very well with the scaling of η_0 in the same concentration range (Fig. 3). The similar dependence on concentration for τ and η_0 suggests that, in the dilute limit, all rheological properties may exhibit a similar dependence on polymer concentration.

For concentrations above c_D, the relaxation time shows a much stronger dependence on polymer concentration ($\tau \sim c^4$). Above c_D, the polymer chains are completely entangled. As the polymer concentration is increased, the number of entanglements also increases. As the number of entanglements increases, the time required to dissipate the energy imparted to the solution also increases as the chains become less mobile due to the entanglements. Boris et al.[55] showed similar results for a well characterized sulfonated polystyrene sample. However, the scaling above c_D for the sulfonated polystyrene was weaker ($\tau \sim c^{1.8}$) than for xanthan due, perhaps, to differences in molecular structure, chain stiffness, or hydrogen bonding.

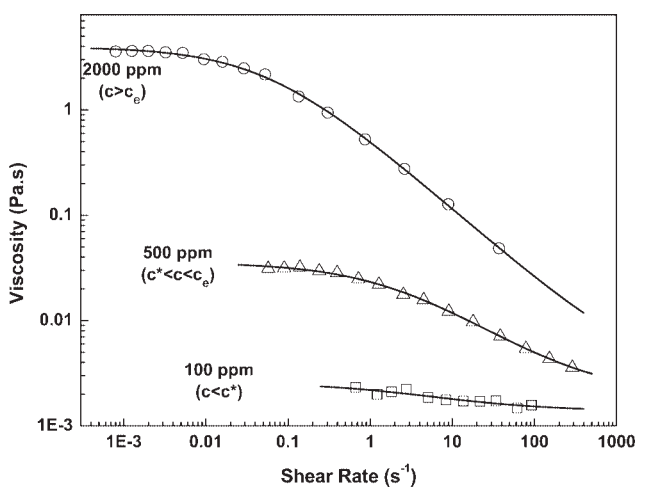

Figure 7 Zero shear rate viscosity dependence on shear rate for several xanthan concentrations in 50 m*M* NaCl. Solid lines represent the Cross model fit to the data.

TABLE II
Fit Parameters for Cross and Power Law Models for Several Xanthan Concentrations in 50 m*M* NaCl

Concentration (ppm)	η_0 (Pa s)	η_∞ (Pa s)	K (s)	m	n
2000	4.0	2.6×10^{-3}	17	0.69	−0.62
500	0.04	1.9×10^{-3}	0.42	0.62	−0.33
100	0.003	1.4×10^{-3}	0.30	0.57	−0.08

Salt solution

For polyelectrolytes, the presence of salt in solution dramatically changes the structure of the polymer in solution which, in turn, changes the rheological properties of the solution. In 50 m*M* NaCl solution, xanthan exhibits shear thinning behavior for concentrations $\sim$ 80 ppm (Fig. 7). As in salt-free solution, the flow curves (Fig. 7) are well described by the Cross model, and the degree of shear thinning (power law index, n) increases with polymer concentration (Table II). For concentrations below c_D (determined in salt-free solution), a sharp decrease in η_0 (up to one order of magnitude) is observed in salt solution. The decrease in viscosity in the presence of salt is commonly observed for polyelectrolytes. The decrease in viscosity is attributed to the salt ions in solution shielding the ionic charges on the polymer chain from one another. The shielding due to the salt ions allows the polymer chain to assume a more compact structure in solution. Because the domains of the polymer chains decrease in size, the number of interactions with neighboring chains also decreases. In other words, more polymer chains are required in solution to get the same amount of intermolecular interaction and subsequent viscosity increase. The relatively strong shear thinning observed at very low polyelectrolyte concentrations ($\sim$ 50 ppm) in salt-free solution is no longer observed in the presence of salt (Fig. 7). In salt solution, xanthan concentrations below 80 ppm were observed to be newtonian.

Critical concentrations for xanthan in 50 m*M* NaCl were determined from a plot of η_0 versus polymer

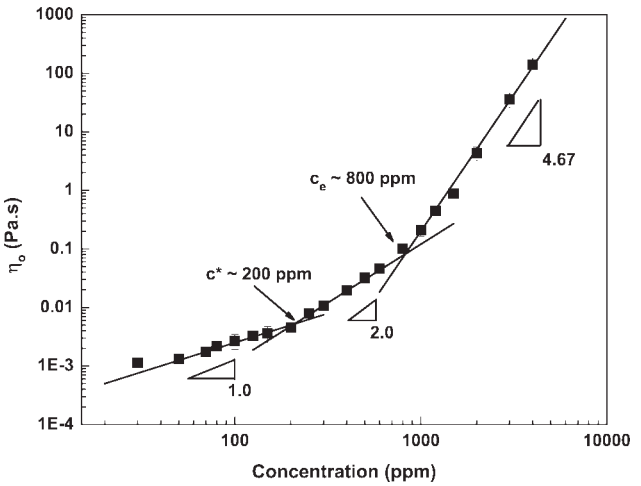

Figure 8 Zero shear rate viscosity scaling dependence on xanthan concentration in 50 m*M* NaCl. Solid lines show scaling predictions for neutral polymers in Θ solvent conditions.

concentration (Fig. 8). When salt is present, three concentration regimes are observed (as opposed to four in salt-free solution). For concentrations above c^*, the dependence of η_0 on concentration is much stronger than in salt-free solution. In the dilute regime, η_0 scales directly with xanthan concentration ($\eta \sim c$). Above c *, the scaling increases to $\eta_0 \sim c^2$. In the semidilute entangled regime, the scaling of η_0 is much stronger with concentration ($\eta_0 \sim c^{14/3}$). Very good agreement with the scaling predictions for a neutral polymer in a Θ solvent was observed in the dilute, semidilute unentangled, and semidilute entangled concentration regimes despite the rigidity of the xanthan chains in salt solution. The measurements confirm the prediction that neutral polymer behavior is observed in the presence of salt. Further, in the presence of NaCl, the abrupt increase in η_0 observed at c^* in salt-free solution was not observed. The less dramatic transition near c^* may be due to the salt ions in solution screening the Coulombic interactions that the polymer experiences in salt-free solution.

An increase in both c^* and c_e is observed in the presence of NaCl. The overlap concentration (~ 200 ppm) is almost three times larger than c^* in salt-free solution (~ 70 ppm). The entanglement concentration (~ 800 ppm) is twice the value of c_e in salt-free solution (~ 400 ppm). The third critical concentration observed in salt-free solution (c_D) is not observed in the presence of NaCl in the polymer concentration range studied here. Because the critical concentrations are dependent on interactions between polymer chains, it follows that solutions of smaller chains would exhibit higher critical concentrations. As stated previously, the salt ions in solution screen the electrostatic interactions between the ions in solution and allow the polymer chains to assume a smaller average configuration. Thus, smaller domain size of the polymer chains corresponds to higher critical concentrations.

The scaling of the relaxation time for xanthan in the presence of salt (Fig. 9) differs markedly from the scaling in salt-free solution. Theory predicts that τ scales as $c^{1/4}$ in the semidilute unentangled regime and as $c^{3/2}$ in the semidilute entangled regime for polyelectrolytes in salt solution. Experimental measurements agree very well with theory in these two concentration regimes. For xanthan concentrations below 80 ppm, the samples are newtonian, therefore no relaxation time can be determined (by definition, $\tau = 0$ for newtonian fluids). For concentrations above 80 ppm in the dilute regime, relaxation time seems to be independent of polymer concentration ($\tau \sim c^0$). The apparent independence of relaxation time in the dilute regime is likely due to the relatively small number of polymer chains present in the solution. Below c^*, the polymer chains do not interact appreciably one with another. Therefore, the relaxation time observed for the solution will be dependent solely on how individual chains react to the stress applied to the solution. The maximum in τ observed for xanthan in salt-free solution (Fig. 6) was not observed in the presence of NaCl. When the polymer concentration is increased above c^*, intermolecular interactions become important, and the result is an increase in the relaxation time (i.e., τ is no longer independent of polymer concentration). Further, the decrease in the magnitude of the relaxation time in both the semidilute unentangled and semidilute entangled regimes is consistent with the fact that the rigid, helical xanthan conformation is stabilized by the presence of salt. The increase in

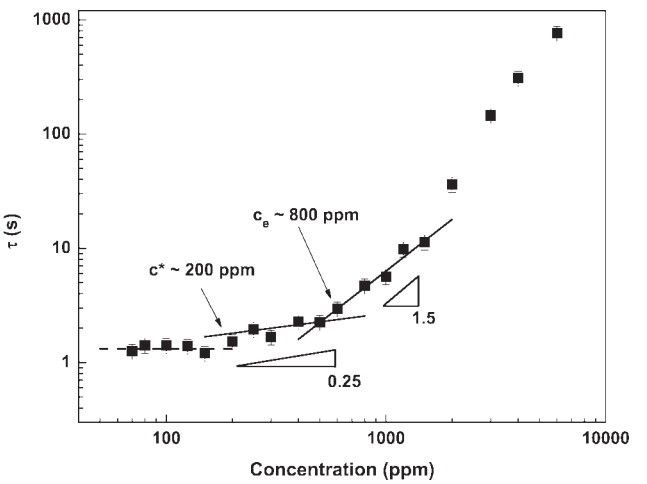

Figure 9 Dependence of relaxation time on xanthan concentration in 50 m*M* NaCl. Solid lines show scaling predicted by theory ($c^* < c < c_D$). Critical concentrations were determined from Figure 8. Error bars represent an estimated error of 15%.

rigidity is expected to be accompanied by a decrease in relaxation time.[57]

The dependence of the relaxation time on polymer concentration begins to deviate from neutral polymer theory at a concentration of 2000 ppm. For concentrations above 2000 ppm, τ scales as $\sim c^3$, which is a weaker dependence than observed for the same concentration range ($c > c_D$) in salt-free solution (Fig. 6). As shown previously, the polyelectrolyte viscosity in 50 m*M* NaCl follows predictions for a neutral polymer in Θ solvent. However, the scaling observed for the relaxation time for polymer concentrations above 2000 ppm in salt-free solution (where neutral polymer behavior is predicted to be observed) differs from that observed in 50 m*M* NaCl in the same concentration region.

CONCLUSIONS

The viscosity of xanthan was measured over seven decades of shear rate and three decades in polymer concentration (10–6000 ppm) in both salt-free and 50 m*M* NaCl solution. For the salt-free solution, the scaling of the zero shear rate viscosity with polymer concentration agrees very well with a simple scaling model for concentrations above c^*. In the presence of salt, the scaling for both the zero shear rate viscosity and the relaxation time differ significantly from the salt-free case. The observed scaling of the zero shear rate viscosity with polymer concentration in 50 m*M* NaCl is well described by theory for neutral polymers in a Θ solvent. In salt-free solution, four concentration regimes are identified with three associated critical concentrations ($c^* \approx 70$ ppm, $c_e \approx 400$ ppm, and $c_D \approx 2000$ ppm). In salt solution, only three concentration regimes and two critical concentrations were observed ($c^* \approx 200$ ppm and $c_e \approx 800$ ppm). The smaller viscosities at the same polymer concentration and larger critical concentrations (c^* and c_e) confirm a collapse in the polymer chains in the presence of salt.

Several findings for the xanthan gum system are not treated by theory and to our knowledge have not been observed in other polyelectrolytes. First, in salt-free solution near c^*, a fivefold increase in the zero shear rate viscosity was observed over a concentration range of $\sim$ 15 ppm. To our knowledge, the dramatic increase in η_0 near c^* has not previously been reported and warrants further experimental and theoretical study. Next, in the salt-free dilute regime, similar dependence was observed for both the zero shear rate viscosity ($\eta_0 \sim c^{1.6}$) and the relaxation time ($\tau \sim c^{1.5}$) suggesting that all rheological properties in the dilute limit may exhibit a similar, nontrivial dependence on concentration. Relaxation time scaling in the salt-free dilute regime follows the expected concentration scaling for neutral polymers in the entangled regime. Third, the semidilute unentangled regime is rather narrow, spanning less than one decade in concentration, which disagrees with predictions that the semidilute unentangled regime spans three to four decades in concentration. Finally, in the entangled concentration regime (above c_D in salt free and above c_e in 50 m*M* NaCl), the scaling of the zero shear rate viscosity shows a greater dependence on concentration in the presence of salt ($\eta_0 \sim c^{15/4}$ in salt free versus $\eta_0 \sim c^{14/3}$ in 50 m*M* NaCl). This work shows that polyelectrolyte scaling theory may apply to rigid polyelectrolytes and flexible ones. Although comprehensive study of chain stiffness and viscosity scaling of polyelectrolytes has not been completed, polyelectrolyte concentration relative to the critical entanglement concentrations seems to be a more important parameter than chain flexibility or rigidity. Additional studies are needed to improve the understanding of viscosity scaling in entangled polyelectrolyte solutions for both flexible and rigid polyelectrolytes.

References

1. Jeanes, A.; Pittsley, J.; Senti, F. R. J Appl Polym Sci 1961, 5, 519.
2. Jansson, P.-E.; Kenne, L.; Lindberg, B. Carbohydr Res 1975, 45, 275.
3. Cuvelier, G.; Launay, B. Carbohydr Polym 1986, 6, 321.
4. Holzwarth, G.; Ogletree, J. Carbohydr Res 1979, 76, 277.
5. Smith, I.; Symes, K.; Lawson, C.; Morris, E. Int J Biol Macromol 1981, 3, 129.
6. Sohn, J.; Kim, C.; Choi, H.; Jhon, M. Carbohydr Polym 2001, 45, 61.
7. Kim, C.; Choi, H.; Kim, C.; Jhon, M. Macromol Rapid Commun 1998, 19, 419.
8. Dentoonder, J.; Hulsen, M.; Kuiken, G.; Nieuwstadt, F. J Fluid Mech 1997, 337, 193.
9. Whitcomb, P. J.; Macosko, C. W. J Rheol 1978, 22, 493.
10. Zirnsak, M.; Boger, D.; Tirtaatmadja, V. J Rheol 1999, 43, 627.
11. Stokke, B.; Elgsaeter, A.; Bjornestad, E.; Lund, T. Carbohydr Polym 1992, 17, 209.
12. Talukdar, M.; Vinckier, I.; Moldenaers, P.; Kinget, R. J Pharm Sci 1996, 85, 537.
13. Ahmed, J.; Ramaswamy, H. J Food Sci Technol 2005, 42, 355.
14. Berth, G.; Dautzenberg, H.; Christensen, B.; Harding, S.; Rother, G.; Smidsrod, O. Macromolecules 1996, 29, 3491.
15. Besio, G.; Leavesley, I.; Prud'homme, R.; Farinato, R. J Appl Polym Sci 1987, 33, 825.
16. Bewersdorff, H.-W.; Singh, R. Rheol Acta 1988, 27, 617.
17. Bezemer, L.; Ubbink, J.; De Kooker, J.; Kuil, M.; Leyte, J. Macromolecules 1993, 26, 6436.
18. Callet, F.; Milas, M.; Rinaudo, M. Carbohydr Polym 1989, 11, 127.
19. Carriere, C.; Amis, E.; Schrag, J.; Ferry, J. J Rheol 1993, 37, 469.
20. Coviello, T.; Burchard, W.; Dentini, M.; Crescenzi, V. Macromolecules 1987, 20, 1102.
21. Holzwarth, G. Biochemistry 1976, 15, 4333.
22. Milas, M.; Rinaudo, M. Carbohydr Res 1986, 158, 191.
23. Rochefort, W.; Middleman, S. J Rheol 1987, 31, 337.
24. Lee, H.-C.; Brant, D. A. Macromolecules 2002, 35, 2212.
25. Lee, H.-C.; Brant, D. A. Macromolecules 2002, 35, 2223.
26. Lee, H.-C.; Brant, D. A. Biomacromolecules 2002, 3, 742.

27. Inatomi, S.-I.; Jinbo, Y.; Sato, T.; Teramoto, A. Macromolecules 1992, 25, 5013.
28. Song, K.-W.; Kim, Y.-S.; Chang, G.-S. Fibers Polym 2006, 7, 129.
29. Mohammed, Z.; Haque, A.; Richardson, R.; Morris, E. Carbohydr Polym 2007, 70, 38.
30. Dobrynin, A. V.; Colby, R. H.; Rubinstein, M. Macromolecules 1995, 28, 1859.
31. Muthukumar, M. J Chem Phys 1997, 107, 2619.
32. Cohen, J.; Priel, Z.; Rabin, Y. J Chem Phys 1988, 88, 7111.
33. Rabin, Y.; Cohen, J.; Priel, Z. J Polym Sci Part C: Polym Lett 1988, 26, 397.
34. Cohen, J.; Priel, Z. Macromolecules 1989, 22, 2356.
35. Vink, H. Polymer 1992, 33, 3711.
36. Roure, I.; Rinaudo, M.; Milas, M.; Frollini, E. Polymer 1998, 39, 5441.
37. Carrington, S.; Odell, J.; Fisher, L.; Mitchell, J.; Hartley, L. Polymer 1996, 37, 2871.
38. Plucktaveesak, N.; Konop, A. J.; Colby, R. H. J Phys Chem B 2003, 107, 8166.
39. Konop, A. J.; Colby, R. H. Macromolecules 1999, 32, 2803.
40. Eckelt, J.; Knopf, A.; Wolf, B. A. Macromolecules 2008, 41, 912.
41. Dou, S.; Colby, R. H. Macromolecules 2008, 41, 6505.
42. Muthukumar, M. Polymer 2001, 42, 5921.
43. Rubinstein, M.; Colby, R. H.; Dobrynin, A. V. Phys Rev Lett 1994, 73, 2776.
44. De Gennes, P.; Pincus, P.; Velasco, R.; Brochard, F. J Phys Fr 1976, 37, 1461.
45. Borsali, R.; Vilgis, T.; Benmouna, M. Macromolecules 1992, 25, 5313.
46. Odijk, T. Macromolecules 1979, 12, 688.
47. Wang, L.; Bloomfeld, V. Macromolecules 1989, 22, 2742.
48. Hara, M. Polyelectrolytes. Science and Technology; Marcel Dekker: New York, 1993.
49. Fuoss, R. Discuss Farad Soc 1951, 11, 125.
50. Milas, M.; Reed, W. F.; Printz, S. Int J Biol Macromol 1996, 18, 211.
51. Sato, T.; Kojima, S.; Narisuye, T.; Fujita, H. Polym J 1984, 16, 423.
52. Sho, T.; Sato, T.; Narisuye, T. Biophys Chem 1986, 25, 307.
53. Ramachandran, R.; Beaucage, G.; Kulkarni, A. S. Macromolecules 2008, 41, 9802.
54. Richardson, R. K.; Ross-Murphy, S. B. Int J Biol Macromol 1987, 9, 257.
55. Boris, D. C.; Colby, R. H. Macromolecules 1998, 31, 5746.
56. Bordi, F.; Cametti, C.; Paradossi, G. Biopolymers 1997, 40, 485.
57. Stockmayer, W. H.; Schmidt, M. Pure Appl Chem 1982, 54, 407.